

# Complexes of the potentially hexadentate ligand bis{3-[6-(2,2'-bipyridyl)]pyrazol-1-yl}hydroborate with representative s-, p-, d- and f-block metal ions: factors promoting formation of mononuclear or double-helical dinuclear complexes

James S. Fleming, Eleftheria Psillakis, Samantha M. Couchman, John C. Jeffery,  
Jon A. McCleverty\* and Michael D. Ward\*†

School of Chemistry, University of Bristol, Cantock's Close, Bristol, UK BS8 1TS

Complexes of the new potentially hexadentate ligand bis{3-[6-(2,2'-bipyridyl)]pyrazol-1-yl}hydroborate ( $L^-$ ), containing two terdentate chelating arms linked by a  $-BH_2-$  spacer, were prepared and crystallographically characterised with  $K^+$ ,  $Cu^{2+}$ ,  $Gd^{3+}$  and  $Tl^+$  as representatives of the s-, d-, f- and p-block metals respectively. The crystal structure of the  $K^+$  complex revealed it to be the double-helical dinuclear  $[K_2L_2]$ , in which each metal ion is six-co-ordinated by a terdentate arm from each of the two ligands; the two ligands are therefore bridging, and folded at the flexible  $-BH_2-$  spacer group. The complex  $[Cu_2L_2][BF_4]_2$  has a similar double-helical dinuclear cation with six-co-ordinate metal centres, but with a greater metal-metal separation because of the greater electrostatic repulsion between two dipositive metal ions compared to  $[K_2L_2]$ . The complex  $[GdL(NO_3)_2]$  in contrast is mononuclear with the ligand co-ordinated in a pseudo-equatorial manner, having a shallow helical twist to avoid steric interference between the terminal pyridyl groups. The two pseudo-axial bidentate nitrate ligands complete the ten-fold co-ordination. Formation of a (triple) helical complex between  $Gd^{3+}$  and  $L^-$ , known with other bis-terdentate compartmental ligands, is thought to be disfavoured in this case because of the electrostatic repulsion between the two +3 metal centres that would occur given the relatively short metal-metal separations imposed by the ligand. In  $[TlL]$  the  $Tl^+$  ion, which is comparable in size and identical in charge to  $K^+$ , has a preference for lower co-ordination numbers, which is reflected in the fact that not all of the ligand binding sites are co-ordinated and there are three relatively short M-N interactions and two long, weak ones.

A recent goal in co-ordination chemistry has been the preparation of architecturally sophisticated, high-nuclearity complexes from self-assembly reactions between potentially bridging multidentate ligands and labile metal ions. The nature of the product depends on the interplay between the properties of both the metal ion (preferences for co-ordination number and/or geometry, charge, size) and the ligand (nature and disposition of metal binding sites, flexibility).<sup>1</sup> Such reactions have resulted in the formation of many beautiful and unusual structures, such as helicates,<sup>2</sup> grids,<sup>3</sup> boxes<sup>4</sup> and rings.<sup>5</sup>

We describe in this paper the preparation of the potentially hexadentate ligand bis{3-[6-(2,2'-bipyridyl)]pyrazol-1-yl}hydroborate ( $L^-$ ). We have recently been studying systematically the synthesis and co-ordination chemistry of polydentate ligands in which two<sup>6</sup> or three<sup>7,8</sup> chelating 'arms' are linked by an appropriate spacer to give flexible ligands with a wide range of co-ordination modes accessible to them, and the study of  $L^-$  is an extension of this work. The crystal structures of its complexes with  $K^+$ ,  $Cu^{2+}$ ,  $Gd^{3+}$  and  $Tl^+$  are presented; this set of metal ions covers every block of the Periodic Table, and also covers a range of sizes and charges. By using such a variety of metal ions with the same ligand we can examine the importance of such factors as metal charge and stereoelectronic preferences on the outcome of the metal/ligand assembly process. Ultimately, information of this sort will allow the development of rational (as opposed to the more usual accidental) synthetic routes towards complex, multinuclear assemblies whose syntheses could not be envisaged by conventional means. A preliminary communication describing the crystal structure of the  $K^+$  complex has recently been published.<sup>9</sup>

## Experimental

### General details

6-Acetyl-2,2'-bipyridine was prepared according to either of the published methods.<sup>10</sup> Other organic reagents and metal salts were obtained from the usual commercial sources and used as received. Instrumentation used for routine spectroscopic analyses has been described earlier.<sup>7,8</sup>

### Preparations

**6-(Pyrazol-3-yl)-2,2'-bipyridine.** (i) A solution of 6-acetyl-2,2'-bipyridine (1.75 g, 8.8 mmol) in dimethylformamide dimethyl acetal (30 cm<sup>3</sup>, a large excess) was heated to reflux for 10 h under  $N_2$  to yield a dark green solution. Removal of the solvent *in vacuo* and recrystallisation of the orange residue from  $CH_2Cl_2$ -hexane afforded the yellow-orange microcrystalline product 1-[6-(2,2'-bipyridyl)]-3-dimethylaminoprop-2-ene-1-one (see Scheme 1) in 76% yield. EI mass spectrum:  $m/z$  254 (100%,  $M^+$ ). <sup>1</sup>H NMR (300 MHz,  $CDCl_3$ ):  $\delta$  8.69 (1 H, d,  $J = 4.4$ , bipy H<sup>6</sup>), 8.52 (2 H, m, bipy H<sup>3</sup> and H<sup>3'</sup>), 8.19 (1 H, d,  $J = 7.6$ ; bipy H<sup>5</sup>), 8.0–7.8 [3 H, m, C(O)CH, and bipy H<sup>4'</sup> and H<sup>5</sup>], 7.33 (1 H, m, bipy H<sup>4</sup>), 6.67 (1 H, d,  $J = 12.8$  Hz, CHN), 3.20 (3 H, s, NMe) and 3.01 (3 H, s, NMe) (Found: C, 70.8; H, 5.9; N, 16.8.  $C_{15}H_{15}N_3O$  requires C, 71.1; H, 6.0; N, 16.6%).

(ii) To a slurry of 1-[6-(2,2'-bipyridyl)]-3-dimethylaminoprop-2-ene-1-one (1.68 g, 6.6 mmol) in EtOH (30 cm<sup>3</sup>) was added hydrazine hydrate (10 cm<sup>3</sup>, a large excess). The mixture was heated to 60 °C in air for 90 min with stirring. The resultant purple solution was cooled, water (180 cm<sup>3</sup>) added, and the mixture refrigerated overnight. A white precipitate separated which was collected by filtration, washed with cold water and pentane, and dried *in vacuo*. Recrystallisation from  $CH_2Cl_2$ -

† E-Mail: mike.ward@bristol.ac.uk

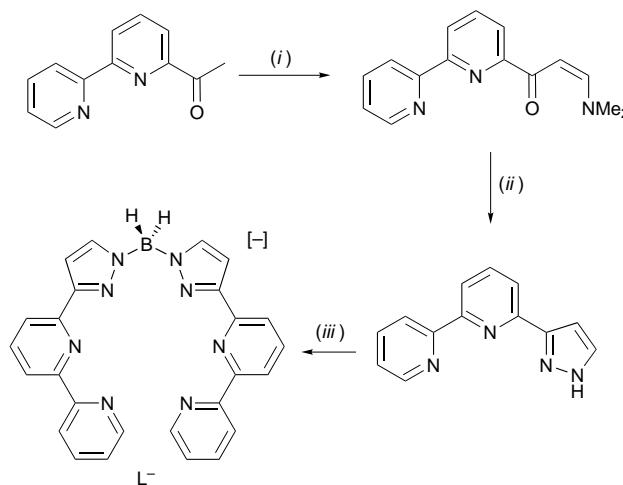
hexane afforded clean 6-(pyrazol-3-yl)-2,2'-bipyridine as a white microcrystalline solid in 72% yield. EI mass spectrum:  $m/z$  222 (100%,  $M^+$ ).  $^1\text{H NMR}$  (300 MHz,  $\text{CDCl}_3$ ):  $\delta$  12.5 (1 H, br s, pyrazolyl NH), 8.76 (1 H, br m, bipy  $\text{H}^6$ ), 8.69 (2 H, m, bipy  $\text{H}^3$  and  $\text{H}^3'$ ), 8.42 (1 H, d,  $J = 7.8$ , bipy  $\text{H}^5$ ), 7.9–8.0 (2 H, m, bipy  $\text{H}^4'$  and  $\text{H}^5$ ), 7.74 (1 H, br s, pyrazolyl  $\text{H}^5$ ), 7.43 (1 H, m, bipy  $\text{H}^4$ ) and 7.05 (1 H, br s, pyrazolyl  $\text{H}^4$ ) (Found: C, 70.0; H, 4.7; N, 25.5.  $\text{C}_{13}\text{H}_{10}\text{N}_4$  requires C, 70.3; H, 4.5; N, 25.2%).

**Potassium bis{3-[6-(2,2'-bipyridyl)pyrazol-1-yl]hydroborate (KL).** A mixture of 6-(pyrazol-3-yl)-2,2'-bipyridine (0.25 g, 1.13 mmol) and  $\text{KBH}_4$  (0.015 g, 0.28 mmol) was ground together finely and then heated slowly under  $\text{N}_2$  to 190 °C. The mixture melted at 120 °C. After 2 h at 190 °C the melt solidified and heating was continued for a further hour. After cooling, warm toluene (50  $\text{cm}^3$ ) was added and the mixture was stirred vigorously for 1 h. The residual white solid was collected by filtration and washed with additional toluene (50  $\text{cm}^3$ ) and then hexane (50  $\text{cm}^3$ ). After air-drying, potassium bis{3-[6-(2,2'-bipyridyl)pyrazol-1-yl]hydroborate was obtained as a white powder (0.057 g, 42%). Negative-ion ES mass spectrum:  $m/z$  455 (100%,  $\text{L}^-$ ) (Found: C, 62.7; H, 4.4; N, 22.2.  $\text{C}_{26}\text{H}_{20}\text{BKN}_8$  requires C, 63.2; H, 4.0; N, 22.7%).  $\nu_{\text{BH}}$  (KBr disc): 2389  $\text{cm}^{-1}$ . X-Ray-quality crystals were grown by slow evaporation of a concentrated solution in  $\text{CHCl}_3$ .

**Other metal complexes.** These were all prepared in the same general manner, by reaction of KL with 1 equivalent of the appropriate metal salt (acetate for  $\text{Mn}^{\text{II}}$ ,  $\text{Cu}^{\text{II}}$ ,  $\text{Zn}^{\text{II}}$  and  $\text{Tl}^{\text{I}}$ ; nitrate for  $\text{Gd}^{\text{III}}$ ) in MeOH at room temperature for 1 h. For the transition-metal complexes a clear solution resulted from which they could be precipitated by addition of aqueous  $\text{NaBF}_4$ ; after filtration and drying *in vacuo* the materials were recrystallised by slow evaporation from MeOH–MeCN, which resulted in X-ray-quality crystals of the copper(II) complex. The neutral complex [TIL] precipitated from the reaction mixture, and was collected by filtration, dried *in vacuo*, and recrystallised from  $\text{CH}_2\text{Cl}_2$ – $\text{Et}_2\text{O}$  by vapour diffusion to give X-ray-quality crystals. The lanthanide complexes  $[\text{ML}(\text{NO}_3)_2]$  ( $M = \text{Ce}$ ,  $\text{Gd}$  or  $\text{Er}$ ) likewise precipitated directly from the reaction mixture and were collected by filtration, dried *in vacuo*, and recrystallised from a dmf–MeCN solution by diffusion of diethyl ether vapour into it. Analytical and mass spectroscopic data for the complex are collected in Table 1.

### X-Ray crystallography

For  $[\text{K}_2\text{L}_2]$ , [TIL] and  $[\text{GdL}(\text{NO}_3)_2]\cdot\text{dmf}\cdot 0.5\text{Et}_2\text{O}$  suitable crystals were quickly transferred from the mother-liquor to a stream of cold  $\text{N}_2$  at  $-100$  °C on a Siemens SMART diffractometer fitted with a CCD-type area detector, and data were collected at  $-100$  °C. Crystals of  $[\text{Cu}_2\text{L}_2][\text{BF}_4]_2\cdot 2\text{MeCN}\cdot 2\text{MeOH}$  lost solvent so fast on removal from the mother-liquor that they decomposed completely during the few seconds it took to transfer them to the cold  $\text{N}_2$  steam. Consequently a suitable crystal was mounted in a sealed glass capillary tube with some of the mother-liquor, and the data were collected at room temperature (use of low temperatures was not possible with the capillary tube as it rapidly became coated with ice). Graphite-monochromatised Mo- $\text{K}\alpha$  radiation was used in all cases. A detailed experimental description of the methods used for data collection and integration using the SMART system has been published.<sup>8</sup> Table 2 contains a summary of the crystal parameters, data collection and refinement. In all cases the structures were solved by conventional direct methods and refined by the full-matrix least-squares method on all  $F^2$  data using the SHELXTL 5.03 package on a Silicon Graphics Indy computer.<sup>11</sup> Absorption corrections were applied using SADABS.<sup>12</sup> Non-hydrogen atoms were refined with anisotropic thermal parameters; hydrogen atoms were included in calculated posi-



**Scheme 1** Synthesis of  $\text{L}^-$  as its  $\text{K}^+$  salt. (i) Dimethylformamide dimethyl acetal, reflux; (ii)  $\text{N}_2\text{H}_4$ , EtOH, reflux; (iii)  $\text{KBH}_4$ , melt

tions and refined with isotropic thermal parameters riding on those of the parent atom. The structural determinations of [TIL] and  $[\text{GdL}(\text{NO}_3)_2]\cdot\text{dmf}\cdot 0.5\text{Et}_2\text{O}$  are of good quality and presented no problems ( $R1 = ca. 0.025$  in each case). Crystals of  $[\text{K}_2\text{L}_2]$ , although they did not suffer from solvent loss, diffracted very poorly: although data were collected to  $2\theta = 55^\circ$ , the data set used in the final refinement was truncated at  $2\theta = 46.5^\circ$  as no significant diffracted intensity was observed beyond that limit, and inclusion of higher angle data resulted in much poorer values of  $R1$  and  $wR2$  with no concomitant improvement in the precision of the structure. The level of refinement for  $[\text{Cu}_2\text{L}_2][\text{BF}_4]_2\cdot 2\text{MeCN}\cdot 2\text{MeOH}$  ( $R1 = 0.050$ ) is reasonable considering the rapid solvent loss and the fact that the structural determination had to be done at room temperature for the reasons outlined above.

CCDC reference number 186/845.

See <http://www.rsc.org/suppdata/dt/1998/537/> for crystallographic files in .cif format.

## Results and Discussion

### $[\text{K}_2\text{L}_2]$

The ligand was prepared by reaction of 6-(pyrazol-3-yl)-2,2'-bipyridine with  $\text{KBH}_4$ , which is the usual route for preparing bidentate bis(pyrazol-1-yl)hydroborates<sup>13</sup> and tridentate tris(pyrazol-1-yl)hydroborates<sup>14</sup> from substituted pyrazoles (Scheme 1). All of the spectroscopic and analytical data were consistent with formation of KL, in which two terdentate N-donor arms are linked by an anionic  $-\text{BH}_2^-$  fragment. Even using a four-fold excess of the pyrazole we found that only the bis(pyrazolyl)borate was obtained, with no trace of the nonadentate tris(pyrazolyl)borate being detectable by either mass spectrometry or IR spectroscopy. The compound was crystallised by slow evaporation from chloroform to give colourless prisms. The crystal structure is shown in Fig. 1, and reveals that in the solid state the compound is in fact a double-helical complex  $\text{K}_2\text{L}_2$ . The double helical structure is emphasised in Fig. 2; bond lengths and angles are in Table 3. A detailed description of the structure was given in the preliminary communication<sup>9</sup> and is therefore not reproduced here, except to note that (i) each  $\text{K}^+$  ion is co-ordinated in an irregular six-co-ordinate environment by two terdentate arms, one from each of the two ligands, with typical K–N separations;<sup>15,16</sup> (ii) the ligand is co-ordinated in a 'strain-free' manner; (iii) overlap of aromatic fragments results in interligand  $\pi$  stacking, a common feature of helicates;<sup>2,17</sup> and (iv) the metal–metal separation [3.954(2) Å] is shorter than that in metallic potassium (4.54 Å) but significantly longer than the sum of two ionic radii for  $\text{K}^+$  ions (*ca.*

**Table 1** Characterisation data for the new complexes

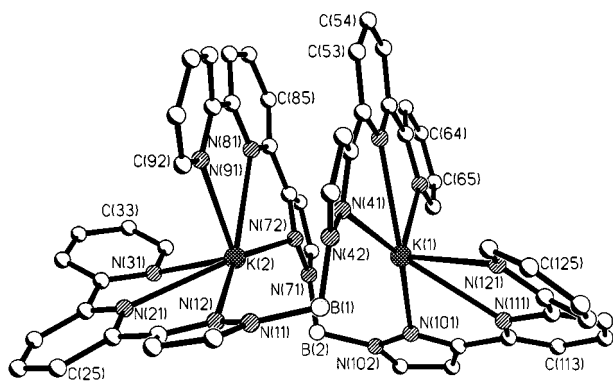
Complex	Yield (%)	Elemental analysis <sup>a</sup> (%)			Mass spectral data <i>m/z</i>
		C	H	N	
[Mn <sub>2</sub> L <sub>2</sub> ][BF <sub>4</sub> ] <sub>2</sub> ·2H <sub>2</sub> O	91	50.5 (50.7)	3.2 (3.6)	18.1 (18.2)	510 [MnL <sup>+</sup> ] <sup>b</sup>
[Cu <sub>2</sub> L <sub>2</sub> ][BF <sub>4</sub> ] <sub>2</sub> ·2H <sub>2</sub> O	64	49.3 (50.0)	3.1 (3.5)	17.6 (18.0)	1124 [Cu <sub>2</sub> L <sub>2</sub> (BF <sub>4</sub> ) <sup>+</sup> ], 518 [Cu <sub>2</sub> L <sub>2</sub> <sup>2+</sup> ] <sup>c</sup>
[Zn <sub>2</sub> L <sub>2</sub> ][BF <sub>4</sub> ] <sub>2</sub> ·2H <sub>2</sub> O	59	49.3 (49.9)	3.3 (3.5)	17.5 (17.9)	1128 [Zn <sub>2</sub> L <sub>2</sub> (BF <sub>4</sub> ) <sup>+</sup> ], 520 [Zn <sub>2</sub> L <sub>2</sub> <sup>2+</sup> ] <sup>c</sup>
[TiL]	48	47.1 (47.3)	3.0 (3.0)	16.7 (17.0)	659 [TiL <sup>+</sup> ] <sup>b</sup>
[CeL(NO <sub>3</sub> ) <sub>2</sub> ]·2H <sub>2</sub> O	72	40.9 (41.3)	2.8 (3.2)	17.9 (18.5)	719 [CeL(NO <sub>3</sub> ) <sub>2</sub> ] <sup>+</sup> <sup>b</sup>
[GdL(NO <sub>3</sub> ) <sub>2</sub> ]·0.5H <sub>2</sub> O	45	41.9 (41.8)	2.6 (2.8)	19.7 (18.8)	675 [GdL(NO <sub>3</sub> ) <sub>2</sub> ] <sup>+</sup> <sup>b</sup>
[ErL(NO <sub>3</sub> ) <sub>2</sub> ]·H <sub>2</sub> O	33	40.2 (40.8)	2.5 (2.9)	18.2 (18.3)	746 [ErL(NO <sub>3</sub> ) <sub>2</sub> ] <sup>+</sup> <sup>b</sup>

<sup>a</sup> Calculated values in parentheses. <sup>b</sup> Fast atom bombardment mass spectrum using 3-nitrobenzyl alcohol as matrix. <sup>c</sup> Electrospray mass spectrum with a cone voltage of 30 V.

**Table 2** Crystallographic data for the four structures

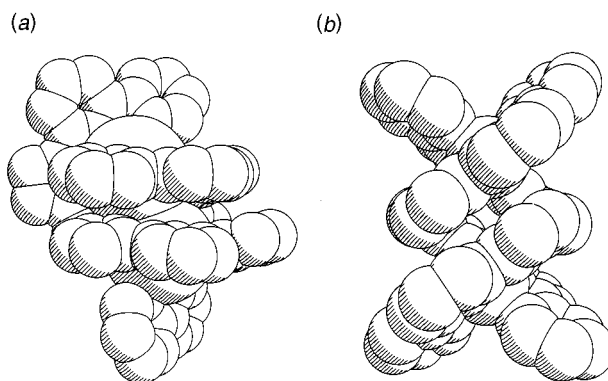
	[K <sub>2</sub> L <sub>2</sub> ]	[Cu <sub>2</sub> L <sub>2</sub> ][BF <sub>4</sub> ] <sub>2</sub> ·2MeCN·2MeOH	[TiL]	[GdL(NO <sub>3</sub> ) <sub>2</sub> ]·dmf·0.5Et <sub>2</sub> O
Formula	C <sub>52</sub> H <sub>40</sub> B <sub>2</sub> K <sub>2</sub> N <sub>16</sub>	C <sub>58</sub> H <sub>53</sub> B <sub>4</sub> Cu <sub>2</sub> F <sub>8</sub> N <sub>18</sub> O <sub>2</sub>	C <sub>26</sub> H <sub>20</sub> BN <sub>8</sub> Tl	C <sub>31</sub> H <sub>32</sub> BGdN <sub>11</sub> O <sub>7.5</sub>
<i>M</i>	988.82	1356.50	659.68	846.74
System, space group	Triclinic, <i>P</i> $\bar{1}$	Triclinic, <i>P</i> $\bar{1}$	Monoclinic, <i>C</i> 2/ <i>c</i>	Triclinic, <i>P</i> $\bar{1}$
<i>a</i> /Å	9.858(2)	13.535(2)	16.608(4)	10.0077(12)
<i>b</i> /Å	13.566(2)	14.600(3)	17.775(4)	13.0213(13)
<i>c</i> /Å	18.4766(12)	19.608(5)	15.910(4)	14.719(3)
$\alpha$ /°	87.541(10)	71.96(2)		70.236(12)
$\beta$ /°	85.050(9)	85.08(2)	90.533(5)	71.349(7)
$\gamma$ /°	83.102(9)	63.362(12)		79.566(8)
<i>U</i> /Å <sup>3</sup>	2442.5(6)	3287.0(12)	4696(2)	1704.6(4)
<i>Z</i>	2	2	8	2
<i>D</i> <sub>c</sub> /g cm <sup>-3</sup>	1.345	1.371	1.866	1.650
$\mu$ /mm <sup>-1</sup>	0.25	0.725	6.912	2.011
<i>F</i> (000)	1024	1386	2544	848
Crystal size/mm	0.4 × 0.25 × 0.1	0.9 × 0.8 × 0.8	0.45 × 0.45 × 0.2	0.4 × 0.3 × 0.3
Reflections collected:	11 128; 6871; 0.0685	33 212; 14 683; 0.0347	18 437; 5356; 0.0385	17 644; 7705; 0.0278
total, independent; <i>R</i> <sub>int</sub>				
2 $\theta$ Limits for data collection/°	3–46.5	3–55	3–55	3–55
Data, restraints, parameters	6616, 0, 665	14 677, 0, 870	5356, 0, 325	7705, 0, 480
Final <i>R</i> 1, <i>wR</i> 2 <sup>a,b</sup>	0.0881, 0.2073	0.0504, 0.1674	0.0253, 0.0521	0.0245, 0.0620
Weighting factors <sup>b</sup>	0.0346, 6.69	0.0846, 0	0.0231, 0	0.0299, 0
Largest peak, hole/e Å <sup>-3</sup>	+0.294, -0.427	0.627, -0.387	+0.819, -1.138	+0.808, -0.617

<sup>a</sup> Structure was refined on *F*<sub>o</sub><sup>2</sup> using all data; the value of *R*1 is given for comparison with older refinements based on *F*<sub>o</sub> with a typical threshold of *F* ≥ 4 $\sigma$ (*F*). <sup>b</sup> *wR*2 = [ $\sum w(F_o^2 - F_c^2)^2 / \sum w(F_o^2)^2$ ]; where *w*<sup>-1</sup> = [ $\sigma^2(F_o^2) + (aP)^2 + bP$ ] and *P* = [max(*F*<sub>o</sub><sup>2</sup>, 0) + 2*F*<sub>c</sub><sup>2</sup>]/3.

**Fig. 1** Crystal structure of [K<sub>2</sub>L<sub>2</sub>]

2.7 Å). The relatively strain-free conformations of the bridge-head -BH<sub>2</sub>- fragment of the ligands is shown by the N-B-N angles, which are 111.0(6) and 110.3(5)° at B(1) and B(2) respectively, very close to the tetrahedral ideal expected in a strain-free conformation.

This complex has several unusual features. First, it is to date the only structurally characterised double-helical complex with an s-block metal. Secondly, the helical geometry of [K<sub>2</sub>L<sub>2</sub>] is not imposed by a preorganised ligand but has arisen naturally from the assembly of achiral ligands around the metal ions, as normally occurs for the transition-metal and lanthanide based helicates.<sup>2</sup> This is in direct contrast to the only other examples of

**Fig. 2** Space-filling representations of (a) [K<sub>2</sub>L<sub>2</sub>] and (b) [Cu<sub>2</sub>L<sub>2</sub>]<sup>2+</sup> emphasising the double-helical ligand arrays and the interligand  $\pi$  stacking

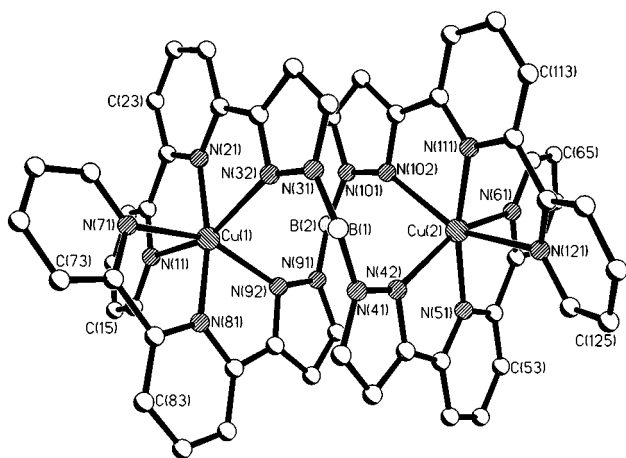
helically chiral complexes with s-block metal ions, in which the ligands are strictly preorganised into helical shapes and therefore inevitably impose helical structures on their complexes.<sup>18,19</sup> It is possible that the 1:1 adduct of 2,2':6',2'':6'',2''':6''',2''''-quinquepyridine (qpy) with LiClO<sub>4</sub> is a double helicate which also arises from a non-preorganised ligand, although structural evidence is lacking in this case.<sup>20</sup> Thirdly, it is an unusual example of alkali-metal co-ordination by an open-chain nitrogen-donor ligand.<sup>16</sup> Alkali-metal complexes with exclusively N-donor ligands usually require highly preorganised ligands

**Table 3** Selected bond lengths (Å) and angles (°) for [K<sub>2</sub>L<sub>2</sub>]

K(1)–N(101)	2.772(5)	K(2)–N(72)	2.766(6)
K(1)–N(41)	2.784(6)	K(2)–N(12)	2.777(6)
K(1)–N(61)	2.816(6)	K(2)–N(91)	2.802(6)
K(1)–N(51)	2.857(5)	K(2)–N(81)	2.855(6)
K(1)–N(111)	2.927(5)	K(2)–N(31)	2.877(6)
K(1)–N(121)	2.956(6)	K(2)–N(21)	2.890(6)
N(101)–K(1)–N(41)	150.1(2)	N(72)–K(2)–N(12)	150.1(2)
N(101)–K(1)–N(61)	84.2(2)	N(72)–K(2)–N(91)	116.3(2)
N(41)–K(1)–N(61)	116.1(2)	N(12)–K(2)–N(91)	85.4(2)
N(101)–K(1)–N(51)	139.3(2)	N(72)–K(2)–N(81)	58.8(2)
N(41)–K(1)–N(51)	59.2(2)	N(12)–K(2)–N(81)	141.5(2)
N(61)–K(1)–N(51)	57.4(2)	N(91)–K(2)–N(81)	58.1(2)
N(101)–K(1)–N(111)	57.3(2)	N(72)–K(2)–N(31)	80.7(2)
N(41)–K(1)–N(111)	134.9(2)	N(12)–K(2)–N(31)	114.4(2)
N(61)–K(1)–N(111)	95.4(2)	N(91)–K(2)–N(31)	105.8(2)
N(51)–K(1)–N(111)	132.5(2)	N(81)–K(2)–N(31)	89.2(2)
N(101)–K(1)–N(121)	111.9(2)	N(72)–K(2)–N(21)	135.8(2)
N(41)–K(1)–N(121)	80.3(2)	N(12)–K(2)–N(21)	59.4(2)
N(61)–K(1)–N(121)	115.3(2)	N(91)–K(2)–N(21)	88.5(2)
N(51)–K(1)–N(121)	97.8(2)	N(81)–K(2)–N(21)	124.7(2)
N(111)–K(1)–N(121)	56.4(2)	N(31)–K(2)–N(21)	56.6(2)
N(42)–B(1)–N(11)	111.0(6)	N(71)–B(2)–N(102)	110.3(5)

**Table 4** Selected bond lengths (Å) and angles (°) for [Cu<sub>2</sub>L<sub>2</sub>][BF<sub>4</sub>]<sub>2</sub>·2MeCN·2MeOH

Cu(1)–N(81)	1.949(3)	Cu(2)–N(51)	1.970(3)
Cu(1)–N(21)	1.977(3)	Cu(2)–N(111)	1.975(3)
Cu(1)–N(71)	2.157(3)	Cu(2)–N(61)	2.179(3)
Cu(1)–N(92)	2.169(3)	Cu(2)–N(42)	2.191(3)
Cu(1)–N(11)	2.275(3)	Cu(2)–N(102)	2.273(3)
Cu(1)–N(32)	2.307(3)	Cu(2)–N(121)	2.278(3)
N(81)–Cu(1)–N(21)	169.08(11)	N(51)–Cu(2)–N(111)	168.44(11)
N(81)–Cu(1)–N(71)	78.15(11)	N(51)–Cu(2)–N(61)	77.67(11)
N(21)–Cu(1)–N(71)	94.02(11)	N(111)–Cu(2)–N(61)	96.70(11)
N(81)–Cu(1)–N(92)	78.95(11)	N(51)–Cu(2)–N(42)	78.31(11)
N(21)–Cu(1)–N(92)	108.48(10)	N(111)–Cu(2)–N(42)	107.40(10)
N(71)–Cu(1)–N(92)	157.06(11)	N(61)–Cu(2)–N(42)	155.84(10)
N(81)–Cu(1)–N(11)	96.11(11)	N(51)–Cu(2)–N(102)	111.56(10)
N(21)–Cu(1)–N(11)	76.76(11)	N(111)–Cu(2)–N(102)	77.64(11)
N(71)–Cu(1)–N(11)	94.60(10)	N(61)–Cu(2)–N(102)	85.27(10)
N(92)–Cu(1)–N(11)	86.49(10)	N(42)–Cu(2)–N(102)	101.25(10)
N(81)–Cu(1)–N(32)	109.55(10)	N(51)–Cu(2)–N(121)	94.07(11)
N(21)–Cu(1)–N(32)	77.60(10)	N(111)–Cu(2)–N(121)	77.67(11)
N(71)–Cu(1)–N(32)	89.10(10)	N(61)–Cu(2)–N(121)	97.94(11)
N(92)–Cu(1)–N(32)	99.82(9)	N(42)–Cu(2)–N(121)	86.28(10)
N(11)–Cu(1)–N(32)	154.28(11)	N(102)–Cu(2)–N(121)	154.21(10)
N(31)–B(1)–N(41)	113.4(3)	N(91)–B(2)–N(101)	112.9(3)

**Fig. 3** Crystal structure of the helical cation of [Cu<sub>2</sub>L<sub>2</sub>][BF<sub>4</sub>]<sub>2</sub>·2MeCN·2MeOH

such as torands,<sup>15,21</sup> macrocycles<sup>22</sup> and cryptands,<sup>23</sup> where the cavity size is a particularly good match for an alkali-metal cation, and the co-ordination geometry is particularly unsuited to a transition-metal ion, neither of which is true in [K<sub>2</sub>L<sub>2</sub>]. It is probable that, considering the predominantly ionic nature of the complex, the affinity of L<sup>−</sup> for K<sup>+</sup> is enhanced by the negative charge of the ligand.

#### First-row transition-metal complexes [M<sub>2</sub>L<sub>2</sub>][BF<sub>4</sub>]<sub>2</sub> (M = Mn, Cu or Zn)

Reaction of [K<sub>2</sub>L<sub>2</sub>] with hydrated metal(II) acetates of Mn, Cu and Zn in a 1:1 M:L ratio, followed by precipitation of the complexes as their tetrafluoroborate salts, afforded in each case a product whose elemental analysis corresponded to the empirical formula [ML][BF<sub>4</sub>]. The electrospray mass spectra indicated that they were dinuclear species, containing strong peaks in each corresponding to [M<sub>2</sub>L<sub>2</sub>(BF<sub>4</sub>)<sub>2</sub>]<sup>+</sup> and [M<sub>2</sub>L<sub>2</sub>]<sup>2+</sup> fragments. In the latter case the *m/z* value for the signal is identical to that which would occur for the monomeric fragment [ML]<sup>+</sup>, but the isotopic patterns and half-integral separations between isotopic components within the signal confirmed the assignment as [M<sub>2</sub>L<sub>2</sub>]<sup>2+</sup>.

The crystal structure of the copper(II) complex (Figs. 2 and 3, Table 4) shows that, like the potassium complex, it is a double-

stranded helicate with each copper(II) ion co-ordinated by one terdentate arm from each of the two ligands. The co-ordination geometry about each metal ion is inevitably irregular because of the bite-angle limitations of the chelating fragments, but the elongation along one axis corresponding to the Jahn–Teller effect is clear: for Cu(1) the (approximately) *trans* pair of donors N(11) and N(32) is more remote than the other four, and for Cu(2) the bonds to N(102) and N(121) are elongated compared to the other four (see Table 4). The usual aromatic  $\pi$ -stacking interactions are present with separations of *ca.* 3.3 Å between overlapping fragments of the two ligands.

The metal–metal separation of 5.388(2) Å is considerably longer than that in the K<sup>+</sup> complex [3.954(2) Å], despite the fact that the ionic radius of Cu<sup>2+</sup> is considerably smaller than that of K<sup>+</sup> as reflected in the M–N distances ( $\approx$ 2.7–2.9 Å for the K<sup>+</sup> complex, 1.9–2.2 Å for the Cu<sup>2+</sup> complex). This presumably reflects the increased intermetal electrostatic repulsion between two dipositive metal ions which will, to a first approximation, be four times greater than that between two monopositive metal ions. Comparison of the two structures shows how the ‘pitch’ of the helical array can be controlled by this electrostatic effect. It has previously been shown by others how the pitch of helicates may also be controlled by steric interactions between substituents on the ligands,<sup>24</sup> and the effects of electrostatic repulsion on the metal–metal separation are apparent in the structures of double-helical complexes of Cu<sup>I</sup>Cu<sup>II</sup> and Cu<sup>II</sup><sub>2</sub> with qpy (metal–metal separations 3.96 and 4.50 Å respectively).<sup>25</sup> The increase in the metal–metal separation is reflected in the increased N–B–N angles [113.4(3) and 112.9(3)° at B(1) and B(2) respectively] which allow the two terdentate fragments within each ligand to stretch further apart from one another at the expense of some additional strain at the bridgehead –BH<sub>2</sub>– groups.

We were interested to see if any magnetic interaction could be detected spectroscopically between the two copper(II) centres. A possible coupling pathway (albeit a rather indirect one) exists through the ligand backbone *via* the –BH<sub>2</sub>– spacer, and a dipolar through-space coupling is also feasible given the relatively short metal–metal separation. The EPR spectrum of a frozen MeCN–thf solution at 77 K (Fig. 4) showed two significant features that suggest a weak through-space coupling between the metal centres. The first is the fact that the copper hyperfine coupling on the main  $\Delta m_s = 1$  transition at *g* = 2.11 is broadened by homogeneous line broadening to the extent where it is barely visible except as a slight irregularity on the

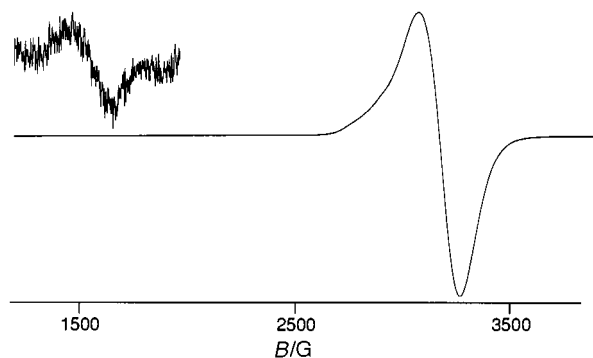


Fig. 4 The X-band EPR spectrum of  $[\text{Cu}_2\text{L}_2][\text{BF}_4]_2$  as a frozen MeCN-thf glass at 77 K;  $G = 10^{-4} \text{ T}$

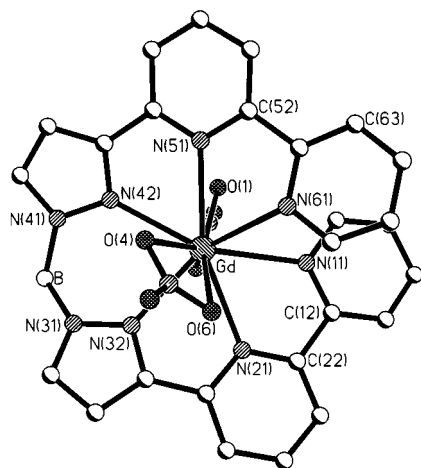


Fig. 5 Crystal structure of the metal complex unit of  $[\text{GdL}(\text{NO}_3)_2] \cdot \text{dmf} \cdot 0.5\text{Et}_2\text{O}$

upward-sloping (low-field) side of the signal. The second is the presence of a very weak  $\Delta m_s = 2$  transition at  $g = 4.29$ . Both of these features are exactly consistent with a weak dipolar interaction transmitted through space.<sup>26</sup> The weakness of the interaction may in part be explained by the relative orientations of the magnetic orbitals as shown from the crystal structure. Assigning the observed elongation to the  $z$  axis, the planes of the magnetic  $d(x^2 - y^2)$  orbitals for each metal are approximately given by the mean planes of the atoms Cu(1)/N(71)/N(21)/N(81)/N(92) and Cu(2)/N(111)/N(51)/N(61)/N(42), which are inclined at  $36^\circ$  to one another. The fact that the magnetic orbitals are approximately parallel to one another in a 'face-to-face' orientation means that overlap between them will be poor.

We also recorded a cyclic voltammogram of the complex to see if any electrochemical interaction between the two metals could be detected from a separation of the  $\text{Cu}^{\text{I}}-\text{Cu}^{\text{II}}$  couples, but the complex underwent only irreversible processes at extreme potentials.

Although we could not obtain X-ray-quality crystals of the other first-row transition-metal complexes, they are clearly also dimeric  $[\text{M}_2\text{L}_2][\text{BF}_4]_2$  complexes and therefore it is reasonable to assume that they are also double helicates.

#### Lanthanide complexes $[\text{ML}(\text{NO}_3)_2]$ ( $\text{M} = \text{Ce}, \text{Gd}$ or $\text{Er}$ )

Given the double helicates formed with two very different metal ions that both had six-fold co-ordination, we were interested to see what sort of structure could arise when  $\text{L}^-$  co-ordinated to lanthanide(III) ions, with their preference for co-ordination numbers of 8–10. Ligands with two terdentate binding domains separated by a flexible spacer have recently been shown to form triple helicates with such metal ions in which the metals are

Table 5 Selected bond lengths ( $\text{\AA}$ ) and angles ( $^\circ$ ) for  $[\text{GdL}(\text{NO}_3)_2] \cdot \text{dmf} \cdot 0.5\text{Et}_2\text{O}$

Gd–N(32)	2.487(2)	Gd–N(21)	2.579(2)
Gd–O(4)	2.488(2)	Gd–N(51)	2.593(2)
Gd–O(1)	2.498(2)	Gd–O(6)	2.602(2)
Gd–N(42)	2.506(2)	Gd–N(61)	2.641(2)
Gd–O(3)	2.519(2)	Gd–N(11)	2.671(2)
N(32)–Gd–N(21)	63.58(8)	N(32)–Gd–N(11)	119.99(7)
N(42)–Gd–N(51)	64.46(7)	N(42)–Gd–N(11)	144.19(7)
N(51)–Gd–N(61)	61.17(7)	N(42)–Gd–N(61)	123.30(7)
N(32)–Gd–N(42)	74.76(8)	N(21)–Gd–N(61)	97.72(7)
N(21)–Gd–N(11)	61.28(7)	N(32)–Gd–N(61)	144.74(8)
N(61)–Gd–N(11)	65.19(7)	N(51)–Gd–N(11)	102.51(7)
N(21)–Gd–N(51)	158.39(8)	N(32)–Gd–N(51)	136.37(8)
N(42)–Gd–N(21)	137.09(8)	O(1)–Gd–O(3)	50.90(6)
O(4)–Gd–O(6)	50.02(6)	N(31)–B–N(41)	110.6(3)

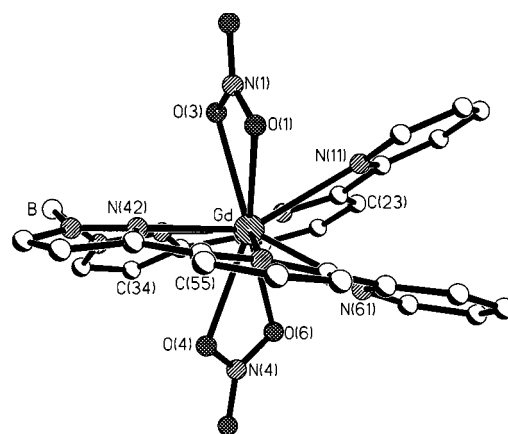


Fig. 6 Alternative 'edge-on' view of the crystal structure of  $[\text{GdL}(\text{NO}_3)_2]$  showing the shallow helical twist of the ligand

nine-co-ordinate, from one terdentate binding pocket of each of three ligands;<sup>27</sup> in contrast, the hexadentate ligand 2,2':6',2''-6'',2'''-6''',2''''-6''''-sexipyridine (spy) forms a mononuclear ten-co-ordinate complex  $[\text{Eu}(\text{spy})(\text{NO}_3)_2]^+$ ,<sup>28</sup> despite its known ability to form helicates with other metal ions in which the ligand becomes partitioned into two terdentate domains.<sup>29</sup>

Reaction of  $[\text{K}_2\text{L}_2]$  with various lanthanide(III) nitrates resulted in formation of complexes whose analytical and mass spectrometric data indicated the formulation  $[\text{ML}(\text{NO}_3)_2]$ . We used a range of lanthanides spanning most of the series and obtained the same result in each case. The crystal structure of  $[\text{GdL}(\text{NO}_3)_2]$  (Figs. 5 and 6, Table 5) shows that the metal ion is ten-co-ordinate, from all six donor atoms of one pseudo-equatorial ligand  $\text{L}^-$ , and four oxygen donors of two pseudo-axial bidentate chelating nitrates. The metal–ligand bond distances are unremarkable. The ligand  $\text{L}^-$  has a shallow helical twist to avoid steric interference between the two terminal pyridyl rings, and the angle between the mean planes of these two pyridyl rings is  $35^\circ$ , emphasised in Fig. 6. The shallow monohelical structure is reminiscent of those of  $[\text{Eu}(\text{spy})(\text{NO}_3)_2][\text{NO}_3]$ <sup>28</sup> and  $[\text{Ag}(\text{qpy})][\text{PF}_6]$ .<sup>30</sup> Bidentate co-ordination of nitrate to lanthanide(III) ions is very common, and there are 24 crystallographically characterised examples for Gd alone in the current version of the Cambridge Structural Database; the Gd–O distances and the bite angle that we observe in  $[\text{GdL}(\text{NO}_3)_2]$  are entirely typical.

The fact that all of the Gd–N bond distances to  $\text{L}^-$  lie within the normal range indicates that the metal ion is a good fit for the cavity formed by the ligand, and helps to account for the structure. However the ionic radii of  $\text{K}^+$  (1.3  $\text{\AA}$ ) and  $\text{Cu}^{2+}$  (0.7  $\text{\AA}$ ) bracket that of  $\text{Gd}^{3+}$  (1.0  $\text{\AA}$ ), yet both of the former form

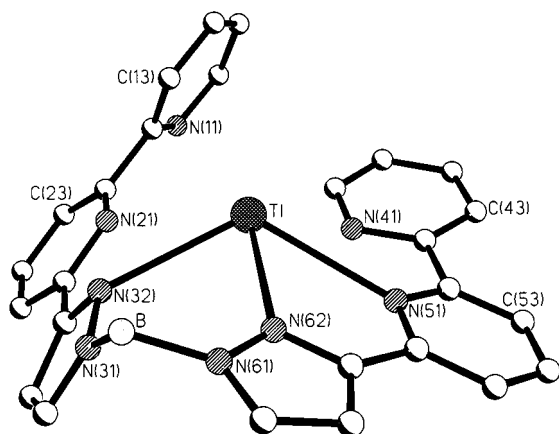


Fig. 7 Crystal structure of [TIL]

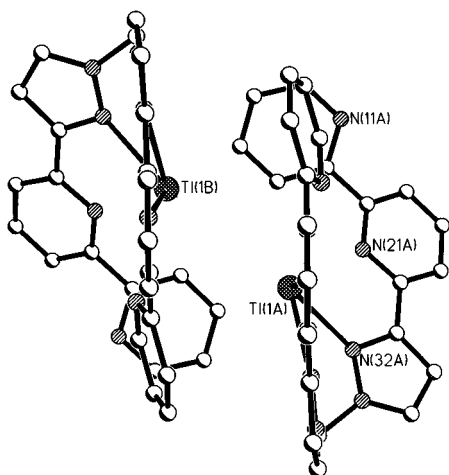


Fig. 8 Stacking between two complex units of [TIL] across an inversion centre

dinuclear helicates whereas the latter does not. Comparison of the two types of structure suggests that the difference between the two structural types cannot arise from any considerations of size compatibility between the metal ion and the ligand cavity, but rather from electrostatic effects. In  $[\text{Cu}_2\text{L}_2]^{2+}$  the increased electrostatic repulsion between two  $\text{Cu}^{2+}$  centres compared to the two  $\text{K}^+$  centres in  $[\text{K}_2\text{L}_2]$  resulted in a considerable increase in the metal–metal separation. For a dinuclear (triple) helicate with  $\text{Gd}^{3+}$  the repulsion would be even more significant and would require a metal–metal separation which this ligand, whose terdentate binding pockets are rather close together, might not be able to accommodate. It is significant that in those dinuclear triple helical complexes known with lanthanide(III) ions the metal–metal separation is in the region of 8 Å as a consequence of the much larger spacer between the two terdentate binding sites.<sup>27</sup>

### [TIL]

Given the formation of a helical complex of  $\text{L}^-$  with  $\text{K}^+$ , we were interested to see what sort of structure would form with an ion of comparable size and charge but which has (i) a preference for lower co-ordination numbers, and (ii) possible stereo-electronic preferences arising from a lone pair of valence electrons which can be stereochemically active.<sup>31</sup> Accordingly the reaction of  $\text{L}^-$  with  $\text{Tl}(\text{CH}_3\text{CO}_2)$  was carried out and the product characterised as mononuclear [TIL]. The crystal structure (Fig. 7, Table 6) shows that the thallium(I) ion is best described as having a '3 + 2' co-ordination geometry, with three strong interactions (arbitrarily defined by comparison with other thal-

Table 6 Selected bond lengths (Å) and angles (°) for [TIL]

Tl–N(62)	2.593(3)	Tl–N(21)	3.389(3)
Tl–N(32)	2.806(3)	Tl–N(41)	3.016(3)
Tl–N(51)	2.866(3)		
N(32)–Tl–N(62)	74.3(1)	N(21)–Tl–N(41)	88.6(1)
N(32)–Tl–N(41)	128.3(1)	N(21)–Tl–N(51)	131.1(1)
N(32)–Tl–N(51)	122.5(1)	N(41)–Tl–N(62)	113.0(1)
N(21)–Tl–N(32)	52.9(1)	N(51)–Tl–N(62)	60.3(1)
N(21)–Tl–N(62)	123.2(1)	N(41)–Tl–N(51)	55.4(1)
N(31)–B–N(61)	109.7(3)		

lium complexes as under 2.9 Å) to N(32), N(62) and N(51), and two weaker interactions with N(21) and N(41) of 3.39 and 3.02 Å respectively. The sixth potential N donor, N(11), is not interacting at all with the  $\text{Tl}^I$ . The pseudo-pyramidal geometry suggests that the lone pair is stereochemically active and completes the (very approximate) tetrahedron that is partially defined by the three stronger Tl–N bonds. Two of the mononuclear units associate by a  $\pi$ -stacking interaction across an inversion centre (Fig. 8), with a separation of ca. 3.5 Å between the parallel overlapping fragments; this association also results in the two thallium(I) ions being brought close together, with a separation of 3.93 Å between them, very similar to the 3.95 Å separation between the  $\text{K}^+$  ions in the helicate  $[\text{K}_2\text{L}_2]$ .

The presence of the short  $\text{Tl} \cdots \text{Tl}$  contact between molecules in the crystal shows that there is no reason on purely electrostatic grounds why  $\text{L}^-$  should not form a double helicate  $[\text{Tl}_2\text{L}_2]$ . However this would require six-fold co-ordination with a relatively hard donor set, which is apparently incompatible with the much 'softer' nature of  $\text{Tl}^+$  compared to  $\text{K}^+$ . In [TIL] the mismatch between the high donor number of the ligand and the preference of the metal ion for low co-ordination numbers has been resolved by some of the potential donor groups not being used, rather than by other possibilities such as two metal ions co-ordinating to one ligand.

### Acknowledgements

We thank the EPSRC for financial support, and Dr. J. P. Maher for recording the EPR spectrum of the copper complex.

### References

- 1 D. Philp and J. F. Stoddart, *Angew. Chem., Int. Ed. Engl.*, 1996, **35**, 1155; D. S. Lawrence, T. Jiang and M. Levett, *Chem. Rev.*, 1995, **95**, 2229; D. B. Amabilino and J. F. Stoddart, *Chem. Rev.*, 1995, **95**, 2725; J.-M. Lehn, *Supramolecular Chemistry*, VCH, Weinheim, 1995.
- 2 E. C. Constable, *Prog. Inorg. Chem.*, 1994, **42**, 67; B. Hasenknopf and J.-M. Lehn, *Helv. Chim. Acta*, 1996, **79**, 1643; C. Piguet, J.-C. G. Bünzli, G. Bernardinelli, G. Hopfgartner and A. F. Williams, *J. Am. Chem. Soc.*, 1993, **115**, 8197; M. Albrecht and O. Blau, *Chem. Commun.*, 1997, 345; R. W. Saalfrank, R. Harbig, J. Nachtrab, W. Bauer, K.-P. Zeller, D. Stalke and M. Teichert, *Chem. Eur. J.*, 1996, **2**, 1363; A. Marquis-Rigault, A. Dupont-Gervais, A. van Dorselaer and J.-M. Lehn, *Chem. Eur. J.*, 1996, **2**, 1395; A. Bilyk, M. M. Harding, P. Turner and P. W. Hambley, *J. Chem. Soc., Dalton Trans.*, 1994, 2783.
- 3 J. C. Jeffery, P. L. Jones, K. L. V. Mann, E. Psillakis, J. A. McCleverty, M. D. Ward and C. M. White, *Chem. Commun.*, 1997, 175; C. Duan, Z. Liu, X. You, F. Xue and T. C. W. Mak, *Chem. Commun.*, 1997, 381; M.-T. Youinou, N. Rahmouni, J. Fischer and J. A. Osborn, *Angew. Chem., Int. Ed. Engl.*, 1992, **31**, 733; P. N. W. Baxter, J.-M. Lehn, J. Fischer and M.-T. Youinou, *Angew. Chem., Int. Ed. Engl.*, 1994, **33**, 2284.
- 4 C. M. Hartshorn and P. J. Steel, *Chem. Commun.*, 1997, 541; P. J. Stang and N. E. Persky, *Chem. Commun.*, 1997, 77; M. Fujita and K. Ogura, *Bull. Chem. Soc. Jpn.*, 1996, **69**, 1471; B. Olenyuk, J. A. Whiteford and P. J. Stang, *J. Am. Chem. Soc.*, 1996, **118**, 8221; P. J. Stang and B. Olenyuk, *Angew. Chem., Int. Ed. Engl.*, 1996, **35**, 732.

- 5 P. L. Jones, K. J. Byrom, J. C. Jeffery, J. A. McCleverty and M. D. Ward, *Chem. Commun.*, 1997, 1361; D. Funeriu, J.-M. Lehn, G. Baum and D. Fenske, *Chem. Eur. J.*, 1997, **3**, 99; B. Hasenknopf, J.-M. Lehn, B. O. Kneisel, G. Baum and D. Fenske, *Angew. Chem., Int. Ed. Engl.*, 1996, **35**, 1838.
- 6 A. M. W. Cargill Thompson, I. Blandford, H. Redfearn, J. C. Jeffery and M. D. Ward, *J. Chem. Soc., Dalton Trans.*, 1997, 2661; D. A. Bardwell, J. C. Jeffery, P. L. Jones, J. A. McCleverty, E. Psillakis, Z. Reeves and M. D. Ward, *J. Chem. Soc., Dalton Trans.*, 1997, 2079; E. Psillakis, J. C. Jeffery, J. A. McCleverty and M. D. Ward, *J. Chem. Soc., Dalton Trans.*, 1997, 1645; K. L. V. Mann, J. C. Jeffery, J. A. McCleverty, P. Thornton and M. D. Ward, *J. Chem. Soc., Dalton Trans.*, 1998, 89.
- 7 P. L. Jones, J. C. Jeffery, J. P. Maher, J. A. McCleverty, P. H. Rieger and M. D. Ward, *Inorg. Chem.*, 1997, **36**, 3088; P. L. Jones, K. L. V. Mann, J. C. Jeffery, J. A. McCleverty and M. D. Ward, *Polyhedron*, 1997, **16**, 2435; A. J. Amoroso, J. C. Jeffery, P. L. Jones, J. A. McCleverty, P. Thornton and M. D. Ward, *Angew. Chem., Int. Ed. Engl.*, 1995, **34**, 1443.
- 8 P. L. Jones, A. J. Amoroso, J. C. Jeffery, J. A. McCleverty, E. Psillakis, L. H. Rees and M. D. Ward, *Inorg. Chem.*, 1997, **36**, 10.
- 9 E. Psillakis, J. C. Jeffery, J. A. McCleverty and M. D. Ward, *Chem. Commun.*, 1997, 479.
- 10 J. E. Parks, B. E. Wagner and R. H. Holm, *J. Organomet. Chem.*, 1973, **56**, 53; E. C. Constable, F. Heirtzler, M. Neuburger and M. Zehnder, *J. Am. Chem. Soc.*, 1997, **119**, 5606.
- 11 SHELXTL 5.03 program system, Siemens Analytical X-Ray Instruments, Madison, WI, 1995.
- 12 SADABS, A program for absorption correction with the Siemens SMART system, G. M. Sheldrick, University of Göttingen, 1996.
- 13 S. Trofimenko, J. C. Calabrese and J. S. Thompson, *Inorg. Chem.*, 1992, **31**, 974 and refs. therein.
- 14 S. Trofimenko, *Chem. Rev.*, 1993, **93**, 943.
- 15 T. W. Bell, P. J. Cragg, M. G. B. Drew, A. Firestone and D.-I. A. Kwok, *Angew. Chem., Int. Ed. Engl.*, 1992, **31**, 345.
- 16 G. Bombieri, G. Bruno, M. D. Grillone and G. Polizzotti, *Acta Crystallogr., Sect. C*, 1984, **40**, 2011.
- 17 E. C. Constable, M. J. Hannon and D. A. Tocher, *J. Chem. Soc., Dalton Trans.*, 1993, 1883.
- 18 T. W. Bell and H. Jousselein, *Nature (London)*, 1994, **367**, 441.
- 19 J. K. Judice, S. J. Keipert and D. J. Cram, *J. Chem. Soc., Chem. Commun.*, 1993, 1323.
- 20 G. Oepen and F. Vögtle, *Liebigs Ann. Chem.*, 1979, 2114.
- 21 T. W. Bell, P. J. Cragg, M. G. B. Drew, A. Firestone, A. D.-I. Kwok, J. Liu, R. T. Ludwig and A. T. Papoulis, *Pure Appl. Chem.*, 1993, **65**, 361.
- 22 E. C. Constable, M. J. Doyle, J. Healy and P. R. Raithby, *J. Chem. Soc., Chem. Commun.*, 1988, 1262.
- 23 J.-M. Lehn and J. B. R. De Vains, *Helv. Chim. Acta*, 1992, **75**, 1221.
- 24 E. C. Constable, M. J. Hannon, A. Martin, P. R. Raithby and D. A. Tocher, *Polyhedron*, 1992, **11**, 2967.
- 25 M. Barley, E. C. Constable, S. A. Corr, R. C. S. McQueen, J. C. Nutkins, M. D. Ward and M. G. B. Drew, *J. Chem. Soc., Dalton Trans.*, 1988, 2655.
- 26 A. Bencini and D. Gatteschi, *EPR of exchange-coupled systems*, Springer, Berlin, 1990.
- 27 C. Piguët, J.-C. G. Bünzli, G. Bernardinelli, G. Hopfgartner and A. F. Williams, *J. Am. Chem. Soc.*, 1993, **115**, 8197; C. Piguët, J.-C. G. Bünzli, G. Bernardinelli, C. G. Bochet and P. Froidevaux, *J. Chem. Soc., Dalton Trans.*, 1995, 83; C. Piguët, G. Hopfgartner, A. F. Williams and J.-C. G. Bünzli, *J. Chem. Soc., Chem. Commun.*, 1995, 491.
- 28 E. C. Constable, R. Chotalia and D. A. Tocher, *J. Chem. Soc., Chem. Commun.*, 1992, 771.
- 29 E. C. Constable, M. D. Ward and D. A. Tocher, *J. Chem. Soc., Dalton Trans.*, 1991, 1675.
- 30 E. C. Constable, M. G. B. Drew, G. B. Forsyth and M. D. Ward, *J. Chem. Soc., Chem. Commun.*, 1988, 1450.
- 31 P. L. Jones, K. L. V. Mann, J. C. Jeffery, J. A. McCleverty and M. D. Ward, *Polyhedron*, 1997, **16**, 2435; D. A. Bardwell, J. C. Jeffery, J. A. McCleverty and M. D. Ward, *Inorg. Chim. Acta*, 1998, **267**, 323 and refs. therein.

Received 4th November 1997; Paper 7/07936B